

Non-ergodic extended phase of the Quantum Random Energy model

Lara Faoro^{1,2}, Mikhail V. Feigel'man^{3,4} & Lev Ioffe^{1,2,5}

Laboratoire de Physique Theorique et Hautes Energies, Sorbonne Universite and CNRS, France

Department of Physics, University of Wisconsin, Madison, USA.

L. D. Landau Institute for Theoretical Physics, Chernogolovka, 142432, Moscow region, Russia

Skolkovo Institute of Science and Technology, Moscow 143026, Russia and

Condensed Matter Physics Laboratory, National Research University "Higher School of Economics", Moscow, Russia

The concept of non-ergodicity in quantum many body systems can be discussed in the context of the wave functions of the many body system or as a property of the dynamical observables, such as time-dependent spin correlators. In the former approach the non-ergodic delocalized states is defined as the one in which the wave functions occupy a volume that scales as a non-trivial power of the full phase space. In this work we study the simplest spin glass model and find that in the delocalized non-ergodic regime the spin-spin correlators decay with the characteristic time that scales as non-trivial power of the full Hilbert space volume. The long time limit of this correlator also scales as a power of the full Hilbert space volume. We identify this phase with the glass phase whilst the many body localized phase corresponds to a 'hyperglass' in which dynamics is practically absent. We discuss the implications of these finding to quantum information problems.

The ergodicity hypothesis states that the dynamic averaging is equivalent to the ensemble averaging with statistical weight.¹ Ergodicity is a common assumption in equilibrium statistical mechanics. However, as it was first shown empirically by Kauzmann in 1948,² the ergodicity hypothesis fails in conventional glasses below the vitrification transition. At temperatures below vitrification the glass is locked into one of many metastable states, so the entropy corresponding to the number of these states does not contribute to the measurable quantities when the system is studied at reasonable times scales. The appearance of the configurational entropy is a distinguishing feature of the glass state and it is firmly established for many classical glass models. Similar phenomenology has been shown in quantum glasses with significant coupling to the environment: as the quantum dynamics is reduced, the system is locked into one of the many metastable states.³ As a result, for both classical glasses and dissipative quantum glasses, it is believed that the glassy state is not completely frozen at all non-zero temperatures and retains some amount of entropy.

Dynamical properties of quantum glasses decoupled from environment are much less understood. Because quantum glasses can be viewed as disordered many body systems, at low temperature they exhibit many body localization⁴, that is the many body equivalent of Anderson localization⁵. In the localized phase their entropy is zero. However, it is not clear whether the quantum glass transition is equivalent to the many body localization, in which the system becomes completely frozen, or it leads to an intermediate phase characterized by non-zero configurational and non-zero dynamically accessible entropies similarly to classical and dissipative quantum glasses. Since mathematically glass models are equivalent to optimization problems, the answer to this question turns out to be relevant for quantum computation where it translates into the estimate of the efficiency of quantum algorithms.

The dynamics of a many body system can be viewed

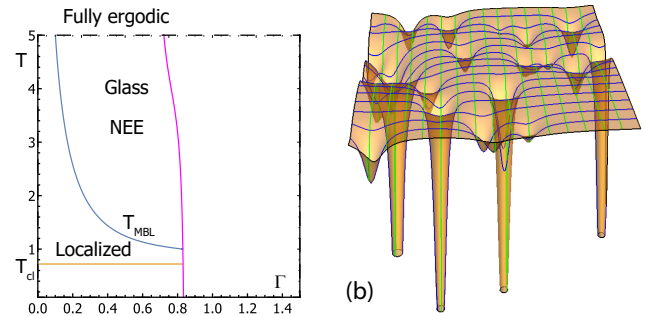


Figure 1: (a) Phase diagram of qREM. Physically, the NEE phase corresponds to the glassy dynamics whilst localized phase corresponds to a completely frozen state, e.g. a hyperglass, see text. (b) Cartoon of 'golf course' potential energy landscape that shows deep uncorrelated minima with very small attraction basins.

as a particle hopping on a graph of states in the Hilbert space.⁶ Recently, a number of works reported the evidence for the existence of non-ergodic delocalized phases for simplified models formulated directly in the Hilbert space, such as disordered random regular graphs⁷⁻¹⁰ and Rosenzweig-Porter (RP)¹¹⁻¹³ models. Evidence for the non-ergodic extended (NEE) phase has been also shown numerically in disordered Josephson junction chains.¹⁴ In all these works, the non-ergodicity was defined as the property of the eigenstates of the Hamiltonian, namely it was shown that the effective volume occupied by these states scales as \mathcal{N}^D where $0 < D < 1$ and \mathcal{N} is the full volume of the Hilbert space. Ergodicity corresponds to $D = 1$. However, the relation between the non-ergodicity defined as the property of the eigenstates and the one defined in glass physics remained unclear.

In this work we fill this gap. Specifically, we study the simplest quantum glass model that can be viewed as

a simplest classical glass in a transverse field. We show that the quantum dynamics of the low energy states can be mapped to the one of the RP model. We focus on the regime of small transverse fields and find three distinct dynamical phases: fully localized one in which the glass is completely frozen (a hyperglass), non-ergodic extended one in which the spin dynamics is slow but does not cease completely (a glass) and fully ergodic paramagnetic state at high temperatures, see Fig. 1a. In addition, the full thermodynamic average displays the low temperature transition from the glass to paramagnetic phases, this transition was discussed in paper¹⁵. We also find that the dynamical spin-spin correlator in the intermediate glassy phase of this model displays the same scaling behavior as the survival probability in the Hilbert space of the RP model studied in papers^{12,13}. Namely, both the dynamic glass order parameter defined by $q = \lim_{t \rightarrow \infty} \langle S(0)S(t) \rangle$ and the survival probability $R(t) = |\langle \Psi(t) | \Psi(0) \rangle|^2$ scale as $q \sim R(\infty) \sim \mathcal{N}^{-D}$.

The fact that in a spin glass the dynamical order parameter and the relaxation time scale as a power of the phase volume \mathcal{N} implies the exponential scaling of these quantities with the number of spins. This is not surprising for low energy states that are separated from each other by large barriers and distances. In fact, similar scaling was reported for the classical dynamics of the p-spin glass in¹⁶.

We note that the problem of quantum dynamics in REM model was considered previously in^{17,18}. This work correctly notices that this model exhibits many body localization transition. However, it incorrectly identifies the phase above MBL transition with the quantum paramagnet. In fact, the dynamics in this phase involves times that scale with the system size. It also uses forward propagation approximation to obtain the the position of MBL line, which cannot be justified in this problem. These mistakes are repeated in the subsequent work¹⁹ on p-spin model.

Model and mapping to RP model.

The model we study is the quantum analogue of the Random Energy Model (REM) introduced for classical glasses in a seminal work²⁰. The Hamiltonian of the qREM reads:

$$H = V(\{\sigma_i^z\}) - \Gamma \sum_{i=1}^n \sigma_i^x = H_{\text{REM}} + H_D \quad (1)$$

$$P(V) = \frac{1}{\sqrt{\pi n}} \exp\left(-\frac{V^2}{n}\right) \quad (2)$$

The degrees of freedom in this model are n spins. As in the REM, $V(\{\sigma_i^z\})$ is a function that takes 2^n different values for the 2^n configurations of the n spins in z-basis, $\{\sigma_i^z\}$. In the following we refer to these spin configurations as spin words. The random potential values are taken randomly from a Gaussian distribution $P(V)$ of

zero mean and variance $n/2$. Despite its simplicity H_{REM} displays many features of the glasses, such as the transition from the paramagnetic state at high temperatures and the low temperature glass state in which the partition function is dominated by the lowest energy state. The transverse field Γ is responsible for the dynamics of the qREM, we consider only $\Gamma < 1$ in this work. The thermodynamical properties of the qREM are also well known^{15,18,21}: at low transverse field, it displays the same transition as the classical model between the paramagnetic and the glass phases. The qREM can be mapped into an Anderson Model on n -dimensional hypercube, where each spin word $\{\sigma_i^z\}$ determines a site with associated onsite energy $V(\{\sigma_i^z\})$. These potential energies are completely uncorrelated in the full $\mathcal{N} = 2^n$ dimensional space. The hopping between nearest neighbor sites is due to the driver Hamiltonian $H_D = -\Gamma \sum_i \sigma_i^x$.

The distinguishing feature of the qREM given in (1 and 2) is the absence of correlations in energy of the states separated by just one spin flip. For the low energy states in the tail of the distribution function $P(V)$ it implies that one spin flip takes the spin state away from the low energy subspace. Qualitatively it corresponds to the energy landscape that consists of rare narrow minima, similar to a golf course with narrow deep holes, such as shown in Fig. 1b. Although unusual for ordinary spin glasses that always display strong correlations between the energies of the states separated by one spin flip, such energy landscape appears in the Number Partitioning Problem that is equivalent to the REM model in the local energy subspace.²² Because the quantum dynamics that starts from one low energy state and leads to another can be viewed as a physical analogue of a quantum search algorithm in a completely structureless problem²³, we expect that the golf course landscape will generally appear in all problems that are equivalent to unstructured searches.

The low temperature behavior of the qREM (1,2) is qualitatively different for small and large Γ : at small Γ the lowest energy states are due to the rare spin configurations for which the potential V is anomalously low, whilst at large Γ they correspond to the spins polarized in x direction. In this work we shall focus on the regime of small $\Gamma \lesssim 1$ for which one expects the glassy behavior. We notice that the quantum glass model (1,2) allows many modifications relevant for the search algorithms; for instance Refs.^{23,24} discussed the one in which $V = 0$ for the majority of the configurations whilst the remaining others are distributed in the narrow band energy around $E_0 \sim n$.

We focus on low temperature regime in which one expects a glassy behavior. At these temperatures the behavior is controlled by the low energy states. A distinguishing feature of the qREM is the presence of two types of low energy states: the states originating from the low energy configurations with anomalously small $V(\{\sigma_i^z\})$ and the states with large polarization in x -direction. It is convenient to discuss them separately. In the absence of Γ , the qREM Hamiltonian reduces to

$V(\{\sigma_i^z\}) = \sum_i^{2^n} V_i |z_i\rangle \langle z_i|$, where we denote with $|z_i\rangle$ the spin states corresponding to the spin words $\{\sigma_i^z\}$. The spacing between the levels at the energy per spin $\epsilon = E/n$ is

$$\delta = \sqrt{\frac{\pi}{n}} \exp(\epsilon^2 - \ln 2) n \quad (3)$$

At $|\epsilon| > \epsilon_c = \sqrt{\ln 2}$ the spacing becomes exponentially large because the spin states at these energies are very rare. In a typical sample there are no states at energies $\epsilon < \epsilon_c$. The temperature at which the partition function is dominated by the lowest state with the energy $\epsilon \approx \epsilon_c$ corresponds to the glass transition in the classical model: $T_c = -1/(2\epsilon_c)$.

The spectrum of the driver Hamiltonian can be written as: $H_D = -\Gamma \sum_{k=1}^{2^n} m_{x_k} |x_k\rangle \langle x_k|$, where m_{x_k} denotes the polarization of the state $|x_k\rangle$. H_D has eigenvalues $\epsilon_m = -\Gamma m$ where $m = -n + 2k$ with integer $k \in (0, n)$. Each discrete level has degeneracy $M(\epsilon_m) = \binom{n}{k} \approx \exp[\ln 2 - m^2/2] n \approx \exp[\ln 2 - \epsilon_m^2/(2\Gamma^2)] n$. Comparing $M(\epsilon)$ with the density of spin states polarized in the z -direction, δ^{-1} given in (3), we see that for $\Gamma < 1/\sqrt{2}$ the states with $\epsilon \ll 1$ are dominated by the classical ones in the limit $n \rightarrow \infty$. The spectrum of polarized states is bound by $\epsilon = \Gamma$, so at very low energies the classical states dominate for $\Gamma < \ln^{1/2} 2$.

At temperatures, $T \gtrsim T_c$ the partition function is controlled by the spin states with energies around $\epsilon = -1/(2T)$. At very low temperature, the spin states are very far from each other, the amplitude of quantum tunneling between them is much smaller than their level spacing, so the quantum states remain fully localized. We term this phase, in which the system remains completely frozen in the low energy classical spin configurations, hyperglass. At higher energies, $\epsilon > \epsilon_A$ Anderson delocalization happens. The transition to the delocalized phase as well as the properties of this phase can be analyzed by mapping the spin problem (1 and 2) to the effective quantum problem of tunneling of low energy spin states caused by the driver Hamiltonian H_D . The resulting effective problem turns out to be equivalent to the RP model.

The tunneling between spin words is due to the driver terms, $\Gamma \sigma_i^x$, in the Hamiltonian. Because the density of the low energy spin states is small, the tunneling between them appear only in high order of the perturbation theory in Γ . We define the distance, d between spin words as the minimal number of spin flips needed to get from one to another. Because the number of the spin words grows exponentially fast with the distance from a given state, the dynamics is dominated by the spin states far away. Indeed, in the leading order of the perturbation theory the amplitude, $H_{ab} = \langle z_a | H | z_b \rangle$ to tunnel the distance d between two spin words corresponding to the spin states $|z_a\rangle$ and $|z_b\rangle$ with energies $E \approx n\epsilon$ is $H_{ab} \sim (\Gamma/n\epsilon)^d d!$ while the number of spin configurations at this distance

increases as $\mathcal{B}(d) \sim n^d/d!$. The condition to find a resonance at distance d , $\mathcal{H}_{ab} \mathcal{B}(d) \sim (\Gamma/\epsilon)^d \sim 1$ is satisfied first at large d indicating that large jumps are most relevant. At large distances the number of spin words that one can attain after d spin flips is $P_d = \binom{n}{d} \approx \exp(n \ln 2 - (d - n/2)^2/2n)$. It has a sharp maximum at $d = n/2$. In the Methods section we show that this dependence is faster than the decrease of the tunneling amplitude with distance, so one can assume that a dominant tunneling process between low energy states occurs due to jumps by distance $d_{\text{typ}} \approx n/2$.

The tunneling between distant spin words can be evaluated by computing such amplitude using only the driver part of the Hamiltonian, i.e. neglecting the effect of the disorder potential on the tunneling. Qualitatively, it means that when computing the tunneling between deep holes in the golf course, Fig. 1b we neglect the effect of the small potential modulation between the deep holes. To justify this assumption we note that the spectrum of the low energy states polarized in x -direction is only weakly affected by the disorder term. Indeed, the degeneracy of the x -polarized states is lifted by the $V(\{\sigma_i^z\})$ term in the Hamiltonian. To estimate this broadening we compute the effective potential projected onto polarized states, $|x\rangle, |x'\rangle$ with the same polarization, m : $V_{xx'} = \langle x | V(\{\sigma_i^z\}) | x' \rangle$. The average value of this potential is zero, $\overline{V_{xx'}} = 0$. The matrix element between two states polarized in z and x -directions is $\langle z | x \rangle^2 = 2^{-n}$, so

$$\overline{V_{xx'}^2} = n 2^{-n-1}. \quad (4)$$

The random potential (4) results in a level width that remains much smaller than the distance between levels with different polarizations:

$$\Delta E = \left[\overline{V_{xx'}^2} M(\epsilon) \right]^{1/2} \sim \exp\left(-\frac{\epsilon_m^2}{4\Gamma^2} n\right) \ll \Gamma/n$$

We conclude that the effect of the $V(\{\sigma_i^z\})$ term on the polarized states is small for the states at low energies.

Crudely, one may estimate the amplitude of the tunneling by distance $d_{\text{typ}} \approx n/2$ by noticing that a typical tunneling process between two spin states, $|z_a\rangle$ and $|z_b\rangle$ at low energies is due to the transitions to highly delocalized states, $|\alpha\rangle$ in the center of the band. The matrix element of this transition is $\langle z_a | \Gamma \sigma^x | \alpha \rangle \sim \langle z_b | \Gamma \sigma^x | \alpha \rangle \sim \Gamma 2^{-n/2}$. Thus, the contribution of a single delocalized state to the transition between $|z_a\rangle$ and $|z_b\rangle$ is $(\Gamma^2/\epsilon n) 2^{-n}$. The transition amplitudes have random signs, so the summation over possible intermediate states gives amplitude $|H_{ab}| \sim 2^{-n/2}$. This estimate neglects the orthogonality of the wave functions of the band center which leads to the suppression of the amplitude for large ϵ . The actual computation that takes into account only the driving terms in the Hamiltonian gives (see below for more details):

$$[(H_{ab})^2]_{\text{typ}} \approx e^{-n[\ln 2 + \phi(\epsilon/\Gamma)]}, \quad (5)$$

where the function

$$\phi(x) = \frac{1}{2} \ln(1-x^2) + \frac{x}{2} \ln \frac{1+x}{1-x} \quad (6)$$

interpolates between $x^2/2$ at small x and $\ln 2$ at $x = 1$. At small x the orthogonality of the wave functions in the center of the band becomes irrelevant, so $\phi(x) \rightarrow 0$ and one reproduces the simple estimate above.

The dominance of the tunneling to the most abundant spin words at a given energy implies that the low energy sector can be mapped into the RP model characterized by a $\mathcal{M} \times \mathcal{M}$ matrix Hamiltonian with independent identically distributed fluctuating matrix elements between the sites, H_{mn} , such that $\overline{(H_{n \neq m})^2} \sim \mathcal{M}^{-\gamma}$ and diagonal matrix elements (bare energies) $\overline{H_{nm}} = 0$, $\overline{(H_{nn})^2} = 1$. At $\gamma > 1$ the off-diagonal matrix elements result in a hybridization of \mathcal{M}^D states with $D = 2 - \gamma < 1$. For this hybridization only the states that are close in energy, $E_a - E_b \sim H_{n \neq m} \ll 1$ are relevant, which implies that the model can be characterized by the typical distance between adjacent bare energies, $\delta \sim \mathcal{M}^{-1}$, instead of the total number of states. The resulting model is defined by $\overline{(H_{n \neq m})^2} \sim \delta^\gamma$. We expect it to be equivalent to RP model for $\gamma > 1$.

At energy ϵ the distance between the energies of the adjacent spin words scales as $\delta \sim \exp(-(\ln 2 - \epsilon^2)n)$ so the low energy states at this energies are equivalent to RP model with

$$\gamma = \frac{\ln 2 + \phi(\epsilon/\Gamma)}{\ln 2 - \epsilon^2} \quad (7)$$

The mapping of the low energy sector to the RP model allows us to establish the presence of two dynamical transitions in the qREM model in addition to the static transition at $\epsilon^2 = \ln 2$. Indeed, the RP model has three distinct phases^{11,12}: for $0 < \gamma < 1$ the system is ergodic and has fractal dimension $D = 1$, for $1 \leq \gamma \leq 2$ the system is in a non ergodic extended phase and has corresponding fractal dimension $D = 2 - \gamma$ and finally for $\gamma > 2$ the system is localized corresponding to fractal dimension $D = 0$. In qREM the transition to the ergodic phase at $\gamma = 1$ occurs at $\epsilon \rightarrow 0$, that is at energies $E \ll n$. We shall not discuss this transition in this work. At all fixed $\epsilon > 0$ the qREM is non-ergodic and it becomes completely localized at $\epsilon < -\epsilon_A$ where ϵ_A is determined by the condition $\gamma = 2$. Note that the position of the MBL transition line is not given by the formula $|\epsilon| \approx \Gamma$ proposed in Refs.^{17,18}.

In the non-ergodic regime the return probability, $R(t) = |\langle \Psi_a(0) | \Psi_a(t) \rangle|^2$, in the equivalent RP model can be found by arguing that off-diagonal matrix elements result in the decay of the initial state with energy E_a into a bath of states with close energies. Such process is irreversible, it is described by a simple exponential relaxation with the relaxation rate

$$1/\tau = \delta^{\gamma-1} \quad (8)$$

At very long time the wave function becomes spread over all states belonging to the same mini-band. As a result, the probability to find the system in the initial state scales as $P \sim \delta^{2-\gamma}$ at long times. Thus one concludes that in RP model the return probability is given by $R(t) \approx e^{-t/\tau} + R_\infty$. This conclusion was verified by simulations¹² and computations¹³. Because the spin configurations at distance $d_{\text{typ}} \approx n/2$ are completely uncorrelated with each other, the same arguments can be applied to the spin-spin correlator:

$$\langle \sigma_i^z(t) \sigma_i^z(0) \rangle \approx \exp(-t/\tau) + q_{EA} \quad (9)$$

$$1/\tau \sim \exp(-\theta n) \quad (10)$$

$$q_{EA} \sim \exp(-\eta n) \quad (11)$$

where

$$\theta = \epsilon^2 + \phi(\epsilon/\Gamma) \quad (12)$$

$$\eta = \ln 2 - 2\epsilon^2 - \phi(\epsilon/\Gamma) \quad (13)$$

In order to verify the predictions (10-13) of the qualitative reasoning we have performed direct simulations of the dynamics of the model (12) in the regime of parameters where one expects to observe the anomalous dimension $0 < D < 1$. The characteristic behavior of the spin-spin correlator obtained in these simulations for $\Gamma = 0.5$ and $T = 1/(2|\epsilon|)$ with $\epsilon = -0.35$ is shown in Fig. 2a. As expected it displays exponential decrease (9) to a constant value. The relaxation rate follows the exponential dependence (10) with the exponent $\theta \approx 0.39$ expected for these parameters. The dynamic spin glass order parameter, q_{EA} also follows exponential size dependence (11) with exponent $\eta \approx 0.1$ that is slightly smaller than the expected value $\eta \approx 0.17$.

The quantum process that starts from the low energy state and leads to another low energy state can be viewed as a solution of the computational problem in which one searches for a state with the full quantum energy that is close to the initial one. The results above imply that it succeeds after time τ given by $\tau = \exp(\theta n)$. The search leads to one of $\exp(\eta n)$ states, so the classical time to find one of such states by brute force search scales as $\tau_{cl} = \exp((\ln 2 - \eta)n)$ multiplied by the time needed to evaluate the quantum energies. Clearly, the quantum time is much shorter than the classical one in whole range of delocalized states, reminiscent of the Grover search²⁵.

Conclusions

The qREM model defined by (12) can be viewed as the simplest many body model that displays localization in its Fock's space. We believe that the appearance of the intermediate non-ergodic state is not an exotic feature but a typical behavior for many body disordered models.

The non-ergodic nature of the wave functions is fragile: broadening of each level that remains non-zero in

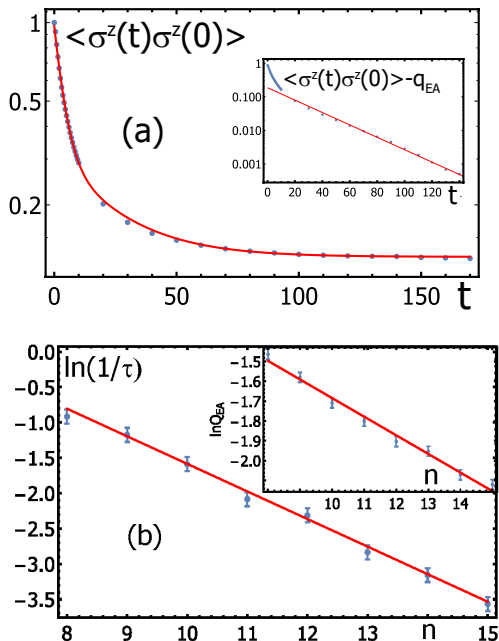


Figure 2: (a) Spin-spin correlator in qREM model (10-13) in non-ergodic delocalized regime corresponding to $\epsilon = -0.35$, $\Gamma = 0.5$ for $n = 14$. The logarithmic plot of $\langle \sigma_i^z(t)\sigma_i^z(0) \rangle - q_{EA}$ shows that it follows exponential dependence (9) over two orders of magnitude. (b) Size dependence of relaxation rate, $1/\tau$ and q_{EA} for $\epsilon = 0.35$, $\Gamma = 0.5$.

the thermodynamic limit destroys it. This has important implication for the recent studies²⁶ that uses random unitary circuit as a toy model for chaotic many body quantum systems. Because random circuit dynamics can be viewed as continuous dynamics with external noise, it is very likely that one cannot observe non-ergodicity in these studies.

Empirically, the classical glasses can be divided into the ones with highly correlated, funnel-like energy landscape and the ones with weak correlations.²⁷ We expect the mapping to RP model to hold for the quantum version of the later at low energies but not for the former. In contrast to the RP dynamics discussed here that is characterized by a single relaxation time, the correlated energy landscape display a continuous spectrum of the relaxation times.

The continuous spectra of relaxation times appears in many glass models in which the barriers between local minima scale with n . In the limit of $n \rightarrow \infty$ at any finite t such glass is trapped in the threshold state characterized by a broad spectrum of relaxation times, the phenomena known as ageing.^{3,28,29} The dynamics discussed in this work occurs in the opposite limit, at the time scales that are exponentially long in n . In this limit the glass is able to explore lower energy states that can be often viewed as deep uncorrelated minima. In particular, it has been shown that classical dynamics of the p-spin model is dominated by the states far in the con-

figuration space separated by the large flat barrier.¹⁶ It is very likely that quantum version of the p-spin model is equivalent to RP.

The relaxation of the a given low energy state can be viewed as a quantum search process. As a result of this search one finds a state which energy is close to the initial one. Because the energies of the initial and final state include quantum corrections, it is not straightforward to translate the results of this search into the algorithm which results can be checked on a classical computer. We leave this question for future work. We note that recent papers³⁰ claiming the solution of this important problem ignore the crucial requirement of the classical verification, constructing thereby, in the words of Scott Aaronson a “computer that simulates itself”.³¹ Other important questions that remain to be addressed are the possibility to implement the qREM Hamiltonian in superconducting circuits in order to solve numerical problems such as NPP and the sensitivity of the results to small coupling to the environment and dissipation.

An interesting corollary of our work are the implications for the quantum information scrambling in many body systems. Because of the non-ergodicity, we expect the appearance of a wide regime in which chaotic dynamics leads to incomplete information scrambling despite the fact that all the regime of non ergodic delocalized states can be viewed as chaotic, characterized by wave function spreading and growth of von Neumann entropy. However, the information is far from being spread uniformly over all allowed states.

A very recent work³⁰ on quantum optimization finds an intermediate phase that it calls “tunneling” but does not realize that it is the spin glass phase characterized by anomalously long times, it also makes incorrect claim that in this phase $q_{EA} = 0$ (i.e. $x = 1/2$ in the notations of³⁰) in contrast with (11). We note that $x = 1/2$ is in the apparent contradiction with the numerical data shown in Fig. 7 of the same work³⁰ that clearly shows $x < 1/2$.

Acknowledgments We are grateful to Boris Altshuler, Kostyantyn Kechedzhi, Vladimir Kravtsov and Vadim Smelyanskiy for useful discussions. The work was partially supported by ARO grant ARO grant W911NF-13-1-0431.

Details of the computation.

Matrix elements: analytic derivation and numerical results

Here we calculate the Green function $G_{ab}^{(0)}(E)$ that determines the transition amplitude between the local (in the z -basis) states a, b with energy E , separated by the distance $d_{ab} = \rho N$ on the hypercube. In this computation we neglect the presence of the random potential V_a ; it can be justified for the contribution to G_{ab} that comes from the x -polarized states with extensive $\sum_i \langle \sigma_i^x \rangle \propto n$ because these states are weakly affected by the random

potential.

We start from the Green function in the imaginary-time representation:

$$\begin{aligned} G^{(0)}(\tau, \rho) &= \prod_i (\cosh \Gamma \tau + \sigma_i^x \sinh \Gamma \tau) = \quad (14) \\ &= \cosh^{N(1-\rho)}(\Gamma \tau) \sinh^{N\rho}(\Gamma \tau) \end{aligned}$$

where we took into account that the product (14) contains exactly $N\rho$ operators σ_i^x . Energy spectrum of the kinetic part of the Hamiltonian is limited to the stripe $E \in (-N\Gamma, +N\Gamma)$. For the energies $E = N\epsilon$ outside of this band (that is, $|\epsilon| > \Gamma$) the Green function can be found from (14) by the Laplace transform and further saddle-point integration (using $N \gg 1$ condition):

$$G^{(0)}(\epsilon, \rho) \approx \exp \left[-NF \left(\frac{\epsilon}{\Gamma}, \rho \right) \right] \quad (15)$$

where

$$F(y, \rho) = y\tau^* - (1 - \rho) \ln \cosh(\tau^*) - \rho \ln \sinh(\tau^*) \quad (16)$$

and the saddle-point value of τ , $\tau_{sp} = \tau^*/\Gamma$ is determined by

$$y = (1 - \rho) \tanh(\tau^*) + \rho \coth(\tau^*) \quad (17)$$

The set of equations (15,16,17) simplifies for the most relevant case of $\rho = \frac{1}{2}$, leading to

$$F \left(y, \frac{1}{2} \right) = y \tanh^{-1} \left(y - \sqrt{y^2 - 1} \right) + \frac{1}{4} \ln(y^2 - 1) + \frac{1}{2} \ln(2). \quad (18)$$

In order to find the Green function at the energies inside the "conduction band", $|\epsilon| < \Gamma$, we employ analytic continuation of (18) over y into the range $|y| < 1$, to obtain the result (5,6).

The analytical computation of the transition amplitude neglects completely the effect of the disorder on the tunneling. In order to check the validity of this approximation, to check the mapping of qREM to RP and establish the parameters of the RP model we performed a number of numerical simulations of qREM model.

First, we computed the time dependent spin-spin correlator and extracted the exponents θ and η that determine the relaxation time, τ , and the spin-glass order parameter. Comparing the numerical results with analytical expectations we conclude that both τ and q_{EA} display exponential dependencies on the system size n as expected (10,11) in the whole non-ergodic phase. The exponents controlling these dependencies are very close to the expected values at energies away from localization transition. However, the difference between expected and observed exponents become significant at low energies. In particular, the localization transition occurs at significantly lower energies than expected analytically indicating larger tunneling amplitudes than the ones given by (5,6). This enhancement of the tunneling amplitude

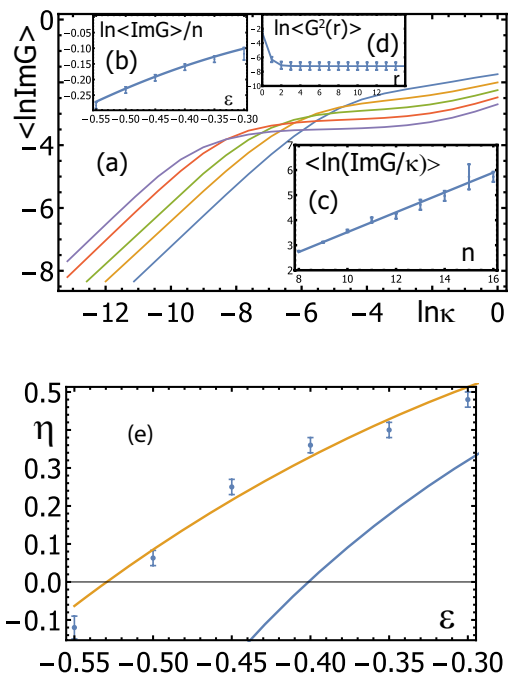


Figure 3: (a) Typical $\Im G(\epsilon, \kappa)$ for $\epsilon = -0.35$, $\Gamma = 0.5$ as a function of κ for $n = 8, 10, 12, 14, 16$. (b) Data for $\langle \Im G(\epsilon, \kappa) \rangle$ and their fit with $\ln \langle \Im G(\epsilon, \kappa) \rangle \approx -0.8n\epsilon^2$. (c) The size dependence of the slope $\ln [\langle \Im G(\epsilon, \kappa) \rangle / \kappa]$ for small κ on the system size n . (d) Green function dependence on the distance. (e) Value of η determined from $d \ln [\langle \Im G(\epsilon, \kappa) \rangle / \kappa] / dn$ and the analytical result corresponding to renormalized $\tilde{\Gamma} = 0.7$ as discussed in the text. The lower line shows the analytical result expected for $\Gamma = 0.5$.

can be viewed as renormalization of the effective Γ that increases the density of polarized states at low energies.

Second, we have computed the diagonal part of $\Im G(\epsilon, \kappa)$ defined by $G(\epsilon, \kappa) = (\epsilon n - H - i\kappa)^{-1}$. The average value of this quantity gives the density of states; it is close to the expected $\ln \langle \Im \text{Tr} G \rangle = -n\epsilon^2$ as shown in Fig. 3. In contrast, the *typical* value of $\Im G(\epsilon, \kappa)$ is controlled by the matrix element that couples a given site to the resonance site at energy $E = -n\epsilon$. At small $\kappa < \delta$, the dominant contribution comes from the spin word that is closest in energy to E , so $\Im G(\epsilon, \kappa)_{\text{typ}} = \kappa [(H_{ab})^2]_{\text{typ}} / \delta^2 \sim \kappa \exp(-n\eta)$, where δ is the level spacing at energy E . At larger $\kappa > \delta$ the dominant contribution comes from many levels and typical value of $\Im G(\epsilon, \kappa)$ saturates at the value given by the Fermi golden rule $\Im G(\epsilon, \kappa)_{\text{typ}} \sim \exp(-n\theta)$. Exactly this behavior is observed numerically, see Fig. 3. However, similar to spin-spin correlator, the precise values of the exponents θ and η determined from these simulations differ somewhat from their analytical values. In particular, the density of states becomes $\nu(\epsilon) = \exp(-c\epsilon^2 n)$ with $c = 0.8$ instead of $c = 1.0$ while faster than expected n -dependence of $\Im G(\epsilon, \kappa)_{\text{typ}}$ indicates renormalization of the effective Γ . For instance, for $\Gamma = 0.5$ the value of η fits well the

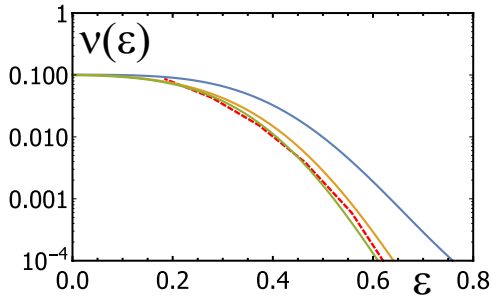


Figure 4: Density of states with large magnetization in x -direction. Two lower full curves show $\nu_{\perp}(\epsilon)$ for $\mu = 0.25$ and $\mu = 0.5$ at $\Gamma = 0.50$. The dashed line shows the density of polarized states expected for $\tilde{\Gamma} = 0.70$. Finally, the upper curve shows the full density of states $\nu(\epsilon)$.

equation $\eta = \ln 2 - 2c\epsilon^2 - \phi(\epsilon/\tilde{\Gamma})$ with $\tilde{\Gamma} \approx 0.7$. For high energies, $\epsilon \gtrsim -0.35$ the values of θ extracted from the $\Im G$ plateau agree very well with the relation $\theta = \ln 2 - c\epsilon^2 - \eta$. Unfortunately it is not possible to check this relation for the whole range of energies because the plateau in $\Im G(\eta)$ is not well defined at low energies for the available sizes $n \lesssim 16$. Finally, the off-diagonal Green function shows very little dependence on the distance for $d \gg 1$ (see

Fig. 3d) that justifies the assumption that the tunneling processes are dominated by hops to large distances $d \sim n/2$.

Third, we have checked directly the renormalization of Γ by studying the density of polarized states defined by $\nu_{\perp}(\epsilon) = \exp(-\mu\epsilon/\tilde{\Gamma}) \text{Tr} \exp(\mu \sum \sigma^x) \Im G(\epsilon)$. The additional factor $\exp(\mu \sum \sigma^x)$ gives extra weight $\exp(\mu m)$ to the states with magnetization m that selects spin states with large magnetizations along x -direction. For instance at $\epsilon = \Gamma$ the contribution of the fully polarized state gets additional factor $\exp(\mu n)$ that overweights the density of classical states $\exp(\ln 2 - \Gamma^2)n$ for $\mu > \ln 2 - \Gamma^2$. The numerical simulation shows that the density of polarized states defined in this way is indeed μ independent and coincides with the one expected for the model with renormalized $\tilde{\Gamma}$ as shown in Fig. 4.

These results make us believe that the presence of intermediate energy states affects the tunneling between the low energy states, which can be described as an increase in the value of $\Gamma \rightarrow \tilde{\Gamma}$. The same hybridization also increases the apparent density of states leading to $c < 1$. In order to exclude the finite size effects we performed a separate study of a modified model in which $V(\{\sigma_i^z\}) = 0$ for most spin words and randomly distributed around $-\epsilon_0$ for others and verified that the renormalization of Γ is absent in this model as expected.²⁴

-
- ¹ L. Boltzmann, *Lectures on gas theory*, vol. Part 2, Chapter 3 (Berkley, 1964).
 - ² W. Kauzmann, *Chem. Rev.* **42**, 219 (1948).
 - ³ L. F. Cugliandolo, *Comptes Rendus Physique* **14**, 685 (2013).
 - ⁴ D. Basko, I. Aleiner, and B. Altshuler, *Annals of Physics* **321**, 1126 (2006).
 - ⁵ P. W. Anderson, *Phys. Rev.* **109**, 1492 (1958).
 - ⁶ B. L. Altshuler, Y. Gefen, A. Kamenev, and L. S. Levitov, *Phys. Rev. Lett.* **78**, 2803 (1997).
 - ⁷ A. De Luca, B. L. Altshuler, V. E. Kravtsov, and A. Scardicchio, *Phys. Rev. Lett.* **113**, 046806 (2014).
 - ⁸ B. L. Altshuler, E. Cuevas, L. B. Ioffe, and V. E. Kravtsov, *Phys. Rev. Lett.* **117**, 156601 (2016).
 - ⁹ V. Kravtsov, B. Altshuler, and L. Ioffe, *Annals of Physics* **389**, 148 (2018).
 - ¹⁰ S. Bera, G. De Tomasi, I. Khaymovich, and A. Scardicchio, *Physical Review B* **98**, 134205 (2018).
 - ¹¹ V. E. Kravtsov, I. M. Khaymovich, E. Cuevas, and M. Amini, *New Journal of Physics* **17**, 122002 (2015).
 - ¹² G. De Tomasi, M. Amini, S. Bera, I. M. Khaymovich, and V. E. Kravtsov, *Survival probability in generalized rosenzweig-porter random matrix ensemble* (2018), URL <http://lanl.arxiv.org/abs/1805.06472>.
 - ¹³ D. Facoetti, P. Vivo, and G. Biroli, *EPL (Europhysics Letters)* **115**, 47003 (2016).
 - ¹⁴ M. Pino, V. Kravtsov, B. Altshuler, and L. Ioffe, *Physical Review B* **96**, 214205 (2017).
 - ¹⁵ Y. Goldschmidt, *Physical Review B (Condensed Matter)* **41**, 4858 (1990).
 - ¹⁶ A. Lopatin and L. Ioffe, *Physical Review B* **60**, 6412 (2007).
 - ¹⁷ C. R. Laumann, A. Pal, and A. Scardicchio, *Phys. Rev. Lett.* **113**, 200405 (2014), URL <https://link.aps.org/doi/10.1103/PhysRevLett.113.200405>.
 - ¹⁸ C. L. Baldwin, C. R. Laumann, A. Pal, and A. Scardicchio, *Physical Review B* **93** (2016).
 - ¹⁹ C. L. Baldwin, C. R. Laumann, A. Pal, and A. Scardicchio, *Phys. Rev. Lett.* **118**, 127201 (2017), URL <https://link.aps.org/doi/10.1103/PhysRevLett.118.127201>.
 - ²⁰ B. Derrida, *Physics Reports* **67**, 29 (1980).
 - ²¹ T. Joerg, F. Krzakala, J. Kurchan, and A. C. Maggs, *Physical Review Letters* **101** (2008).
 - ²² H. Bauke, S. Franz, and S. Mertens, *Journal of Statistical Mechanics: Theory and Experiment* **2004**, P04003 (2004).
 - ²³ V. N. Smelyanskiy, K. Kechedzhi, S. Boixo, S. V. Isakov, H. Neven, and B. Altshuler, *Non-ergodic delocalized states for efficient population transfer within a narrow band of the energy landscape* (2018), URL <http://lanl.arxiv.org/abs/1802.09542>.
 - ²⁴ V. N. Smelyanskiy, K. Kechedzhi, H. Neven, and B. Altshuler (2018).
 - ²⁵ L. Grover, *Physical Review Letters* **79**, 325 (1997).
 - ²⁶ C. W. von Keyserlingk, T. Rakovszky, F. Pollmann, and S. L. Sondhi, *PHYSICAL REVIEW X* **8** (2018).
 - ²⁷ C. Angell, *Science* **319**, 582 (2008).
 - ²⁸ L. Cugliandolo and J. Kurchan, *Physical Review Letters* **71**, 173 (1993).
 - ²⁹ J.-P. Bouchaud, L. Cugliandolo, J. Kurchan, and M. Mezard, *Physica A* **226**, 243 (1996).
 - ³⁰ C. L. Baldwin and C. R. Laumann, *Phys. Rev. B* **97**, 224201 (2018), URL <https://link.aps.org/doi/10.1103/PhysRevB.97.224201>.

1103/PhysRevB.97.224201.

³¹ S. Aaronson, private communication.